Biosensors and Bioelectronics 157 (2020) 112177

Contents lists available at ScienceDirect

Biosensors and Bioelectronics

journal homepage: http://www.elsevier.com/locate/bios

SiRNA-directed self-assembled quantum dot biosensor for simultaneous detection of multiple microRNAs at the single-particle level

Fei Ma [1], Su Jiang [1], Chun-yang Zhang [*]

College of Chemistry, Chemical Engineering and Materials Science, Collaborative Innovation Center of Functionalized Probes for Chemical Imaging in Universities of Shandong, Key Laboratory of Molecular and Nano Probes, Ministry of Education, Shandong Provincial Key Laboratory of Clean Production of Fine Chemicals, Shandong Normal University, Jinan, 250014, China

ARTICLE INFO

Keywords:
Quantum dot
Fluorescent biosensor
MicroRNA
Single-particle detection
SiRNA

ABSTRACT

MicroRNAs are essential post-transcriptional regulators and may act as the noninvasive biomarkers for disease diagnosis. Sensitive and multiplexed detection of microRNAs may facilitate the accurate and early clinical diagnosis, but the available methods are usually compromised by using organic dyes as the signal probes, laborious chemical and enzymatic manipulations, and the complicated reaction schemes. Here we reported a siRNA-directed self-assembled quantum dot (QD) biosensor for facile and simultaneous detection of multiple microRNAs. In this biosensor, the binding of microRNA targets with corresponding QD nanoprobes leads to the formation of siRNA duplexes, which not only induces the spectrally resolved coding of microRNAs, but also facilitates the assembly of QDs:magnetic nanoparticle bioconjugates for the isolation and enrichment of target microRNAs. The disassembled QDs can be sensitively detected by single-molecule detection, enabling quantitatively sensing of microRNAs at the single-particle level. This biosensor employs only QDs as the signal reporters, which can simultaneously detect multiple microRNAs from the same sample and achieves femtomolar sensitivity and single-base mismatch selectivity without the involvement of any target labeling and amplification steps. Moreover, it can be successfully applied for simultaneous detection of circulating microRNAs in clinical serum samples, holding great potential in non-invasive early diagnosis and biomedical researches.

1. Introduction

MicroRNAs are evolutionarily conserved non-coding RNAs with short length (Bartel, 2004). As crucial post-transcriptional regulators, microRNAs can efficiently repress target gene expression through mRNA cleavage or translational repression (Huntzinger and Izaurralde, 2011) and play key roles in different stages of life cycle including development (Wienholds et al., 2005), differentiation (Yi et al., 2008), and aging (Xu et al., 2003). The aberrant microRNA expression may inevitably disturb the normal gene regulation network to cause a variety of human diseases such as diabetes (Kantharidis et al., 2011), myocardial disease (Thum et al., 2008), neurodegenerative disease (Hébert and De Strooper, 2009), and cancers (Calin and Croce, 2006), and the circulating microRNAs in peripheral blood have emerged as potential biomarkers for non-invasive disease diagnosis (Mitchell et al., 2008). Especially, multiple microRNAs can jointly regulate a single gene function, and a single type of disease may be associated with the deregulation of various different microRNAs (Porkka et al., 2007). Therefore, the simultaneous detection of multiple microRNAs is of great importance to biomedical research and clinical practices. The microRNA microarray (Thomson et al., 2004), quantitative reverse transcription-polymerase chain reaction (qRT-PCR) (Kroh et al., 2010), and isothermal nucleic acid amplification (Deng et al., 2017) are the most popular approaches for microRNA assay. Nevertheless, the requirements for direct labeling of microRNA molecules, multiple DNA probes and enzymes, and laborious procedures may increase the assay cost and complexity (Kilic et al., 2018; Shen et al., 2015). Moreover, organic dyes (e.g. SYBR Green, Cy3, Cy5, FAM, and TAMARA) are frequently used as the signal reporters in the microRNA assays, but they suffer from poor photostability, low quantum yield, narrow absorption, broad red-tailed emission, and small Stokes shift, which may inevitably compromise the assay accuracy, repeatability and multiplexing capability (Li et al., 2014).

Semiconductor quantum dots (QDs) are ideal alternatives to organic dyes due to their high quantum yield, excellent photochemical stability,

* Corresponding author.
E-mail address: cyzhang@sdnu.edu.cn (C.-y. Zhang).
[1] These authors contributed equally.

https://doi.org/10.1016/j.bios.2020.112177
Received 31 January 2020; Received in revised form 16 March 2020; Accepted 24 March 2020
Available online 26 March 2020

and large Stokes shift (Medintz et al., 2005; Resch-Genger et al., 2008; Stanisavljevic et al., 2015). Particularly, the broad excitation and sharp size-tunable emission enables the simultaneous excitation of multiple QDs with a single wavelength, making QDs suitable for multiplexed biosensing Geiβler et al. (2010); Han et al. (2001); Jaiswal et al. (2003); (Song et al., 2015). Nevertheless, most of QD-based biosensors still require organic dyes to achieve fluorescence resonance energy transfer for target detection (Hildebrandt et al., 2017), and the limitations of organic dyes cannot be excluded. Moreover, unlike long nucleic acids such as DNAs and RNAs (Ho et al., 2005), the use of QDs for direct microRNA detection is extremely difficult because the short length of microRNA is insufficient to form a stable base pairing with the detection probes. To overcome this barrier, a QD-based time-gated method is developed for microRNA assay by exploiting base stacking effect, but it requires the careful optimization of the lengths and orientations of both Tb- and QD-labeled probes (Qiu and Hildebrandt, 2015). Alternatively, several indirect nucleic acid amplification approaches are introduced to convert microRNA signal to long DNA signal (Hu et al., 2018; Ma et al., 2019), but the involvement of multiple enzymes and detection probes complicates the experimental design and increases the assay cost. Therefore, the application of QDs for simple, direct and simultaneous detection of microRNAs remains to be explored.

2. Materials and methods

2.1. Materials and reagents

All RNA oligonucleotides (Supplementary information, Table S1) were synthesized and HPLC purified by TaKaRa Biotechnology (Dalian, China). The 605QDs (2 μM), the 655QDs (1 μM), and the magnetic rack (DynaMag™-Spin) were obtained from Invitrogen (Carlsbad, CA, USA). Chitin magnetic microparticles (MMPs) and the chitin-binding domain (CBD)-fused p19 protein were purchased from New England Biolabs (Beverly, MA, USA). The miRNeasy RNA isolation kit was obtained from Qiagen (Valencia, CA, USA). Sodium chloride (NaCl), ethylenediamine tetraacetic acid (EDTA), Tween-20 and tris (2-carboxyethyl) phosphine hydrochloride (TCEP, 0.5 M, pH 7.0), and bovine serum albumin (BSA) were purchased from Sigma-Aldrich (St. Louis, MO, USA). Sodium dodecyl sulfate (SDS, 10% (w/v)), 4 × Tris-HCl (0.5 M, pH 6.8), RNase-free water were obtained from Sangon Biological Engineering Technology and Service Company (Shanghai, China).

2.2. Buffer solution

1 × MMP pretreatment buffer (100 mM NaCl, 1 mM EDTA, 1 mM TCEP, 1 mg/mL BSA, and 20 mM Tris-HCl, pH 7.0); 10 × p19 Binding Buffer (1 M NaCl, 10 mM EDTA, 10 mM TCEP, 0.2% (v/v) Tween-20, and 200 mM Tris-HCl, pH 7.0); 1 × wash buffer (100 mM NaCl, 1 mM EDTA, 100 μg/mL BSA, and 20 mM Tris-HCl, pH 7.0); 1 × elution buffer (100 mM NaCl, 1 mM EDTA, 1 mM TCEP, 0.5% SDS, and 20 mM Tris-HCl, pH 7.0).

2.3. Pretreatment of MMPs and preparation of the QD probes

The MMPs were pretreated to reduce non-specific binding: First, 500 μL of suspension of chitin MMPs was transferred into a sterile microfuge tube, and the MMPs were pulled to the side of the tube using a magnetic rack to remove the supernatant. Second, 500 μL of MMPs-pretreatment buffer was added to the tube, and the suspension was stirred vigorously and the supernatant was removed. Finally, 500 μL of fresh MMPs-pretreatment buffer was added, and the tube was rotated at 40 rpm for 4 h. The resultant chitin MMPs were used immediately or stored at 4 °C for at least 4 months. The QD probes were prepared by incubating equal molar ratio of QDs and the corresponding anti-microRNA probes at room temperature for 30 min.

2.4. MicroRNA detection

The 30 μL of hybridization solution containing target microRNA with indicated concentrations, 2.5 μL of chitin MMP, 0.2 U/μL p19 protein, 1 × p19 binding buffer, 1 mg/mL BSA, and 30 nM QD probes were incubated at room temperature for 30 min. After the hybridization, the supernatant was removed, and the resultant MMPs were extensively washed with 1 × washing buffer for three times. Finally, the captured QD probes were disassembled by denaturation of p19 using 1 × elution buffer containing 0.5% SDS and subjected to single-particle detection.

2.5. Circulating microRNA detection

The peripheral blood samples of nonsmall cell lung cancer (NSCLC) patients and the healthy persons were obtained from the Affiliated Hospital of Guangdong Medical University (Zhenjiang, Guangdong, China), and the experiments were approved by the ethics committee of the Affiliated Hospital of Guangdong Medical University. The plasma was isolated from blood samples by centrifuging whole blood at 3000 rpm for 20 min. The total RNA was extracted from 500 μL of plasma using the Qiagen miRNeasy RNA isolation kit according to the manufacturer's protocol. The final volume used to elute total RNA was 30 μL, and the amount of total RNA was determined by the NanoDrop 2000c Spectrophotometer (Thermo Scientific, Wilmington, Delaware, USA). For circulating microRNA detection, the total RNA was added to 30 μL of solution containing 2.5 μL of chitin MMP, 0.2 U/μL p19 protein, 1 × p19 binding buffer, 1 mg/mL BSA, and 30 nM QD probes, and incubated at room temperature for 30 min. After the hybridization, the supernatant was removed, and the resultant MMPs were extensively washed with 1 × washing buffer for three times. Finally, the captured QD probes were disassembled by denaturation of p19 with 1 × elution buffer containing 0.5% SDS and subjected to single-particle detection.

2.6. Single-particle detection

The inverted Olympus IX-71 microscope (Olympus, Tokyo, Japan) was used for TIRF imaging-based single-particle detection. A sapphire 488 nm laser (50 mW, Coherent, USA) was used to simultaneously excite the 605QDs and the 655QDs. The emitted photons were collected by an oil immersion 100 × objective (Olympus, Japan) and imaged onto the two halves of an Andor Ixon DU897 EMCCD camera (Andor, Belfast, UK) with an exposure time of 100 ms. An image series of 10 frames were acquired from a single slide. All the images were analyzed by the Image J software (NIH, Bethesda, MD, USA). The size of particles was set at 2–20 pixels to reduce the false positive signals generated from the noises. For data analysis, a region of interest (ROI) with 600 × 600 pixels was selected for single-particle counting.

2.7. Gel electrophoresis

To analyze the binding of p19 with siRNA, the products were analyzed by 8% nondenaturating polyacrylamide gel electrophoresis in 1 × TBE buffer (9 mM boric acid, 0.2 mM EDTA, and 9 mM Tris-HCl, pH 7.9) at 100 V constant voltages for 45 min in an ice bath. The resultant gel was imaged by a ChemiDoc™ MP Imaging System (Bio-Rad, Hercules, CA, USA).

3. Results and discussion

3.1. Principle of the proposed biosensor

The RNA silencing mediated by small-interfering RNA (siRNA) is a crucial cellular defence mechanism against viral infections, and some viruses encode RNA silencing suppressor protein to block the RNA silencing process (Silhavy et al., 2002). The p19 is a well-characterized RNA silencing suppressor that can specifically bind siRNA with higher

affinity (K_d = 0.17 nM) than single-stranded RNA (K_d > 2000 nM) (Ye et al., 2003). Superior to the traditional sandwich hybridization assay that is unsuitable for the recognition of short length target due to the unstable base-paring (Qiu and Hildebrandt, 2015), the p19 enables direct and highly stable capturing of short microRNA sequences. Moreover, the binding of p19 with siRNA is sequence-independent (Vargason et al., 2003), thus multiple microRNAs can be simultaneously recognized by p19 without the requirement of complicated detection probes design and optimization. In this research, we report a novel siRNA-directed self-assembled QD biosensor for simultaneous detection of multiple microRNAs at the single-particle level (Scheme 1). As a proof of concept, miR-155 and miR-21 are used as the target microRNAs, both of which are promising cancer biomarkers (Habbe et al., 2009; Si et al., 2007). This assay involves four reagents including two QD probes, a p19 protein, and a magnetic microparticle (MMP). The QD probes are constructed by the conjugation of single-stranded RNA to two spectrally distinguishable QDs (Supplementary information, Fig. S1), with the 605QD probe being complementary to miR-155 and the 655QD probe being complementary to miR-21 (Figs. S2 and S3). The p19 is fused with the chitin-functionalized chitin-binding domain (CBD), and the MMP is functionalized with chitin. Therefore, the p19 can bind to MMP surface via specific CBD-chitin interaction (Chong et al., 1997). The QDs-siRNAs-p19-MMP bioconjugates can be self-assembled by one-step mixing of target microRNAs with QD probes, p19, and MMP. Specifically, miR-155 and miR-21 can hybridize with the 605QD probe and the 655QD probe to form 605QD-siRNA 1 and 655QD-siRNA 2, respectively. The two QDs-siRNAs can simultaneously bind with p19 through electrostatic recognition, facilitating their assembly on the MMP to form the QDs-siRNAs-p19-MMP bioconjugates. These bioconjugates enable simultaneous coding, enrichment and isolation of multiple microRNAs from complex biological samples. Upon the denaturation of p19 by sodium dodecyl sulfate (SDS) (Bhuyan, 2010), the QDs probes are disassembled from the MMP. The free QDs can be simultaneously detected via single-particle counting. This assay requires only the QDs as the signal reporters and can be completed through self-assembly process without the requirement of any chemical/enzyme reactions, allowing simultaneous detection of multiple microRNAs from a single sample. With the assistance of single-molecule detection technique, this biosensor can achieve femtomolar sensitivity with single-base selectivity, and it can be further applied for detection of lung cancer-related circulating microRNAs in clinical serum.

3.2. Verification of the binding of p19 with the QDs-siRNAs

We used gel mobility shift assay to verify the binding of p19 with the QDs-siRNAs. As shown in Fig. 1A, an obvious gel shift band of p19-605QD-siRNA 1 complex is observed when p19, miR-155 and 605QD probe coexist (lane 2), indicating the binding of p19 with 605QD-siRNA 1. In contrast, in the absence of miR-155 (lane 3), p19 protein (lane 4), or both of miR-155 and p19 protein (lane 1), the p19-605QD-siRNA 1 band disappears, and only the bands of 605QD probe (lanes 1 and 3) and 605QD-siRNA 1 (lane 4) are observed. Similar results are observed in the case of miR-21 (Fig. 1B). An obvious gel shift band of p19-655QD-siRNA 2 complex can be observed only in the presence of p19, miR-21, and 655QD probe (lane 2), but this band disappears in the absence of miR-21 (lane 3), p19 (lane 4), or both miR-21 and p19 (lane 1). These results clearly demonstrate that the p19 protein can efficiently bind with the QD-siRNAs, enabling specific capture of QD probes only when the corresponding target microRNAs are present.

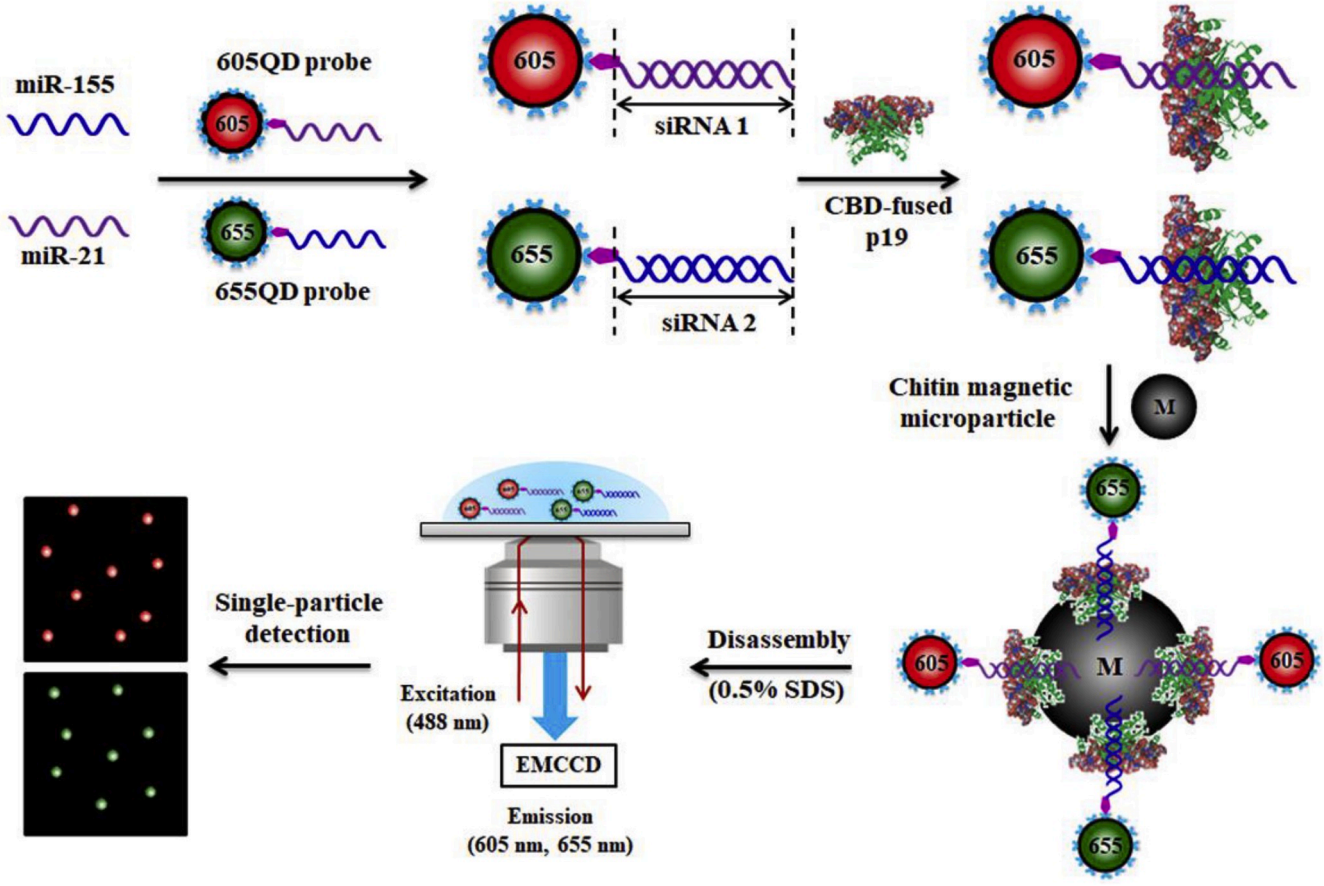

Scheme 1. Schematic illustration of the self-assembled QD biosensor for multiplex microRNA assay.

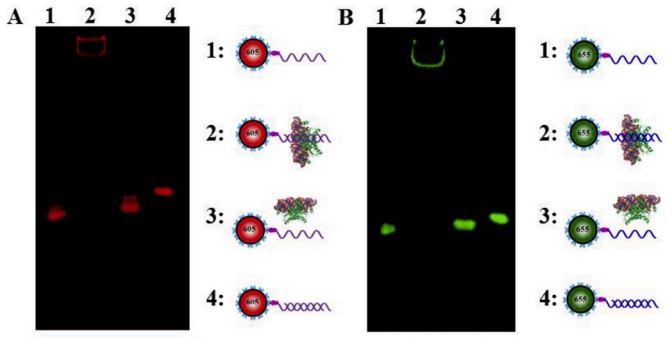

Fig. 1. (A) Gel mobility shift analysis of the binding of p19 with 605QD-siRNA 1. Lane 1: 605QD probe; Lane 2: p19 + miR-155 + 605QD probe; Lane 3: p19 + 605QD probe; Lane 4: miR-155 + 605QD probe. (B) Gel mobility shift analysis of the binding of p19 with the 655QD-siRNA 2. Lane 1: 655QD probe; Lane 2: p19 + miR-21 + 655QD probe; Lane 3: p19 + 655QD probe; Lane 4: miR-21 + 655QD probe. The 605QD signal is shown in red (A), and the 655QD signal is shown in green (B). (For interpretation of the references to colour in this figure legend, the reader is referred to the Web version of this article.)

3.3. Detection of microRNA at the single-particle level

The nucleic acid amplification methods can greatly improve microRNA assay sensitivity (Deng et al., 2017; Kroh et al., 2010), but the involvement of different enzymes and special templates/primers inevitably increases the assay cost and tends to induce false positivity resulting from nonspecific amplification. Single-molecule detection has significant advantages of high sensitivity (from attomole to femtomolar) and low sample consumption over conventional ensemble measurements (Ma et al., 2016), making it ideal for the quantification of low-abundant targets. In this research, we used single-molecule detection to quantify the QDs signal (Supplementary information, Fig. S4). After hybridization for 1 h (Supplementary information, Fig. S5), the resultant free QDs are subjected to single-molecule detection (Supplementary information, Fig. S6). In the presence of miR-155 alone, only the 605QD signals are detected (Fig. 2B) and no 655QD signal is observed (Fig. 2F). In the presence of miR-21 alone, only the 655QD signals can be detected (Fig. 2G) but no 605QD signal is detected (Fig. 2C). In contrast, there is neither 605QD signal (Fig. 2A) nor 655QD (Fig. 2E) signal in the absence of miR-155 and miR-21. Moreover, upon the addition of miR-155 and miR-21, both 605QD (Figs. 2D) and 655QD (Fig. 2H) fluorescence signals can be simultaneously detected. These results clearly demonstrate that the assembly and disassembly of QDs: MMP nanocomplexes can be used for simultaneous detection of multiple microRNAs (Supplementary information, Fig. S6). Notably, superior to the organic dyes-based single-molecule detection (Yang and Zhang, 2013) which requires different lasers to separately excite different fluorescent molecules, the broad excitation and narrow emission of QDs allows for the performance of this assay in a single-excitation and dual-emission manner, greatly simplifying the instrument setup and experimental procedures (Chu et al., 2016).

3.4. Detection sensitivity

We further evaluated the sensitivity of the proposed biosensor by measuring the QD counts in response to different concentrations of target microRNAs. As shown in Fig. 3A, the 605QD counts gradually enhance as a function of the increase of miR-155 concentration from 0 to 2×10^{-10} M, and a linear correlation is obtained between the 605QD counts and the miR-155 concentration from 1×10^{-13} to 1×10^{-11} M with a regression equation of $Y = 6.425 + 3.647X$ ($R^2 = 0.9991$), where Y is the 605QD counts and X is the miR-155 concentration (pM). Moreover, the 655QD counts improve as a function of miR-21 concentration from 0 to 1×10^{-10} M, and a linear correlation is obtained between the 655QD counts and the miR-21 concentration from 1×10^{-13} to 1×10^{-11} M with a regression equation of $Y = 17.61 + 15.17X$ ($R^2 = 0.9986$), where Y represents the 655QD counts and X represents the miR-21 concentration (pM) (Fig. 3B). These results demonstrate that the proposed method has a broad dynamic range of $1 \times 10^{-13} - 2 \times 10^{-10}$ M for miR-155 and $1 \times 10^{-13} - 1 \times 10^{-10}$ M for miR-21, respectively, and high sensitivity with a limit of detection of 100 fM (or 3 amol, Supplementary information, Fig. S7) for both miR-155 and miR-21. Notably, 100 fM microRNAs can be well discriminated from the control group without target, and the sensitivity has been improved by 4 orders of magnitude compared with that of organic dye-based molecular beacon method (1 nM) (Baker et al., 2011) and is even comparable to the duplex-specific nuclease signal amplification method (100 fM) (Yin et al., 2012), suitable for the detection of microRNA in clinical samples (Wang et al., 2011). The high sensitivity of this method can be ascribed to (1) the efficient coding of target microRNAs by QDs to convert the microRNA signal to distinct QD signal, (2) extremely low background

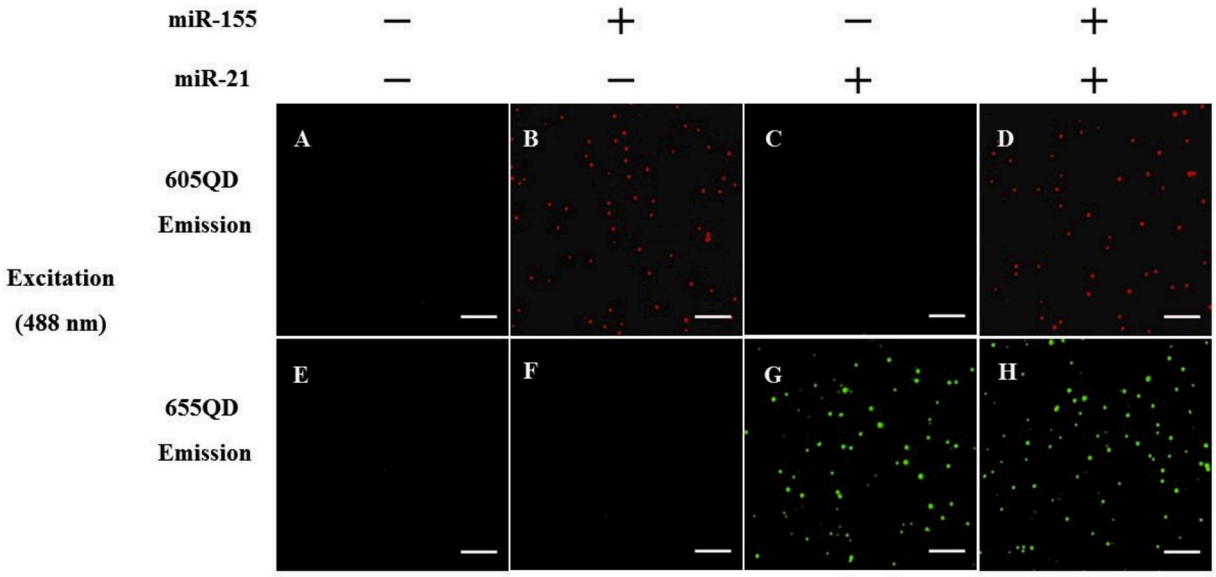

Fig. 2. Simultaneous detection of miR-155 and miR-21 at the single-particle level. The signal of 605QD is shown in red, and the signal of 655QD is shown in green. The scale bar is 5 μm. (For interpretation of the references to colour in this figure legend, the reader is referred to the Web version of this article.)

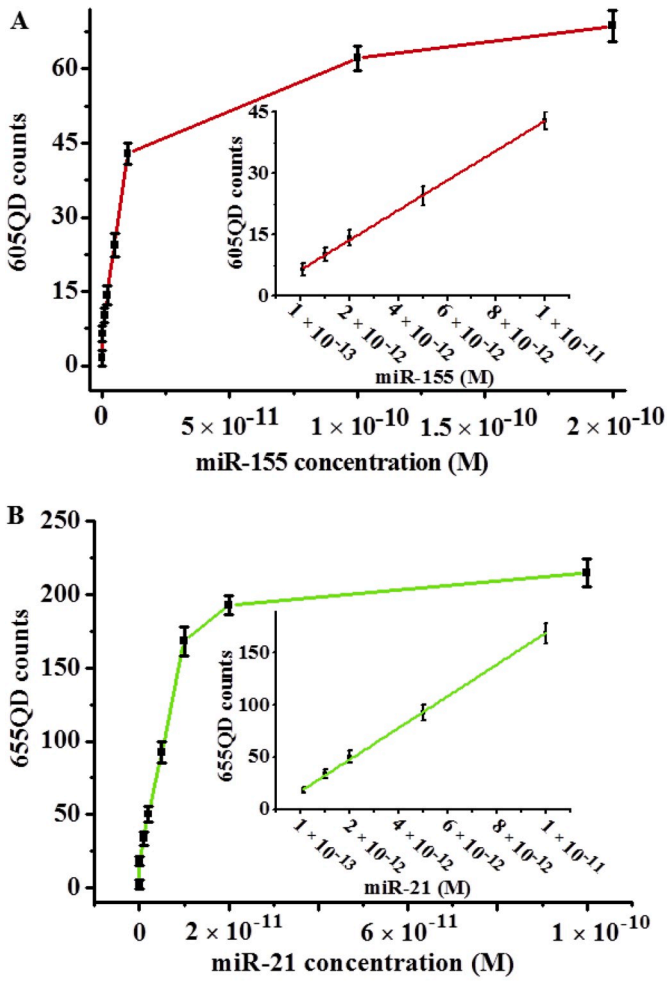

12

Fig. 3. (A) Variance of 605QD counts as a function of miR-155 concentration. Insert shows the calibration curve of 605QD counts versus miR-155 concentration. (B) Variance of 655QD counts as a function of miR-21 concentration. Insert shows the calibration curve of 655QD counts versus miR-21 concentration. Error bars show the standard deviation of three experiments.

signal due to the introduction of magnetic isolation, and (3) inherent high signal-to-noise of single-molecule detection technique.

3.5. Assay specificity

We used the single-base mismatched microRNA targets M-miR-155 and M-miR-21 (Fig. 4A) to investigate the specificity of the proposed biosensor. As shown in Fig. 4B, only a low background signals of 605QD and 655QD is observed in the control group without any target microRNA. In contrast, a high 605QD fluorescence signal is observed in the presence of only miR-155, and a high 655QD fluorescence signal is detected in the presence of only miR-21. Moreover, the 655QD and 605QD fluorescence signals can be simultaneous detected when both miR-155 and miR-21 coexist. Especially, the signal of miR-155 is 2.77-fold higher than that of M-miR-155, and the signal of miR-21 is 7.03-fold higher than that of M-miR-21, indicating that even single-base difference can be well discriminated by the proposed biosensor. The high selectivity of the proposed biosensor can be ascribed to different binding affinity of p19 protein to the fully complementary siRNA and mismatched siRNA, which can be verified by the gel mobility shift analysis of the binding of p19 protein with the QD-labeled siRNAs. As

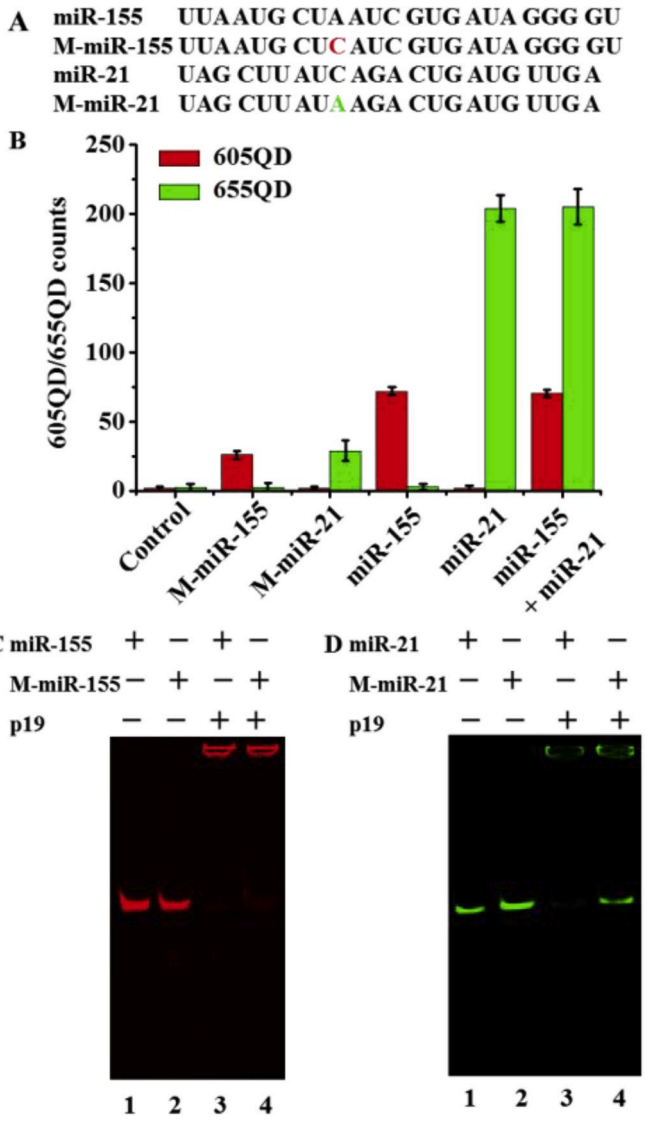

Fig. 4. (A) Sequences of miR-155, M-miR-155, miR-21 and M-miR-21, with the single-base variation being shown in red. (B) Variance of the 605QD and the 655QD counts in response to M-miR-155, M-miR-21, miR-155, miR-21, the co-existence of miR-155 and miR-21, and the control group without any target microRNA. The concentrations of each microRNA is 50 pM. Error bars show the standard deviation of three experiments. (C) Gel mobility shift analysis of the binding of p19 with the 605QD-labeled siRNA 1. Lane 1: miR-155 + 605QD probe; Lane 2: M-miR-155 + 605QD probe; Lane 3: miR-155 + p19 + 605QD probe; Lane 4: M-miR-155 + p19 + 605QD probe. (D) Gel mobility shift analysis of the binding of p19 with the 655QD-labeled siRNA 2. Lane 1: miR-21 + 655QD probe; Lane 2: M-miR-21 + 655QD probe; Lane 3: miR-21 + p19 + 655QD probe; Lane 4: M-miR-21 + p19 + 655QD probe. (For interpretation of the references to colour in this figure legend, the reader is referred to the Web version of this article.)

shown in Fig. 4C, similar siRNA band was produced in the presence of either miR-155 (Fig. 4C, lane 1) or M-miR-155 (Fig. 4C, lane 2), indicating that the single-base difference in miR-155 does not affect the formation of siRNA. With the addition of p19 protein, the distinct gel shift band of p19-605QD-siRNA complexes can be observed due to the binding of p19 with the 605QD-labeled siRNA 1 (Fig. 4C, lanes 3 and 4). Notably, in comparison with the group of miR-155 (Fig. 4C, lane 3), much more siRNA left after binding with p19 in the group of M-miR-155 (Fig. 4C, lane 4), indicating that p19 has lower affinity towards the mismatched siRNA 1. Similarly, in comparison with miR-21, M-miR-21 does not affect the formation of siRNA 2 (Fig. 4D, lanes 1 and 2), but

leads to much more siRNA 2 left after binding with p19 (Fig. 4D, lanes 3 and 4). Notably, the different signal enhanced rates between miR-155 and miR-21 groups may be ascribed to diverse binding affinity caused by their different sequences and lengths. These results demonstrate that the use of p19 as the recognition element enables the accurate detection of microRNA with single-base mismatch selectivity.

3.6. Detection of circulating microRNAs

To verify the feasibility of the proposed biosensor for simultaneous detection of circulating microRNAs, we measured miR-155 and miR-21 in serum of nonsmall cell lung cancer (NSCLC) patients and healthy donors. Both miR-155 (Fig. 5A) and miR-21 (Fig. 5B) levels in the patient samples are significantly higher than those in normal samples (Student's t-test, $P < 0.001$). The mean levels of miR-155 and miR-21 in the lung cancer group are increased by 5.43-fold and 1.55-fold, respectively, compared with those of healthy group. These results are consistent with the previous report that the levels of serum miR-155 (Wang et al., 2011) and miR-21 (Liu et al., 2012) in lung cancer patients are significantly higher than those in healthy volunteers. These results clearly demonstrate that the proposed biosensor can be applied for simultaneous detection of circulating microRNAs, providing a new powerful platform for cancer research and non-invasive diagnosis.

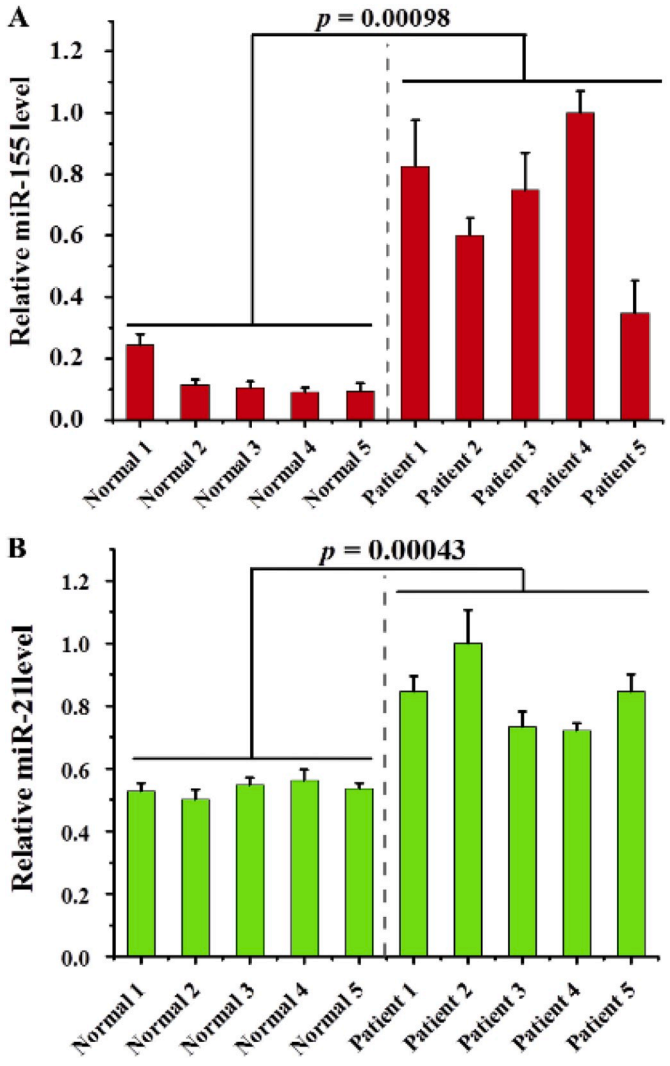

Fig. 5. Simultaneous detection of circulating miR-155 (A) and miR-21 (B) in serum from normal peoples and the NSCLC patients. Error bars show the standard deviation of three experiments.

4. Conclusions

In summary, we have demonstrated the use of siRNA-directed self-assembled QDs biosensor for simultaneous detection of multiple microRNAs. In this assay, one-step mixing of the reagents (i.e., the QD probes, p19, and the MMP) with target microRNAs can induce the assembly of the QDs-siRNAs-p19-MMP bioconjugate, enabling simultaneous coding, enrichment, and isolation of multiple microRNAs from a single sample. Upon the denaturation of p19 by SDS, the QDs are disassembled from the MMP and simply quantified by single-particle counting. This biosensor does not involve any organic dyes and chemical/enzyme reactions, greatly simplifying the experimental design and reducing the assay cost. With the introduction of single-particle detection, the proposed biosensor enables direct measurement of microRNAs with femtomolar sensitivity and single-base discrimination capability, and it can be applied for simultaneous detection of multiple circulating microRNAs in clinical samples. Moreover, the proposed biosensor can be easily extended to the multiplexed detection of more than two microRNAs targets by employing more than two kinds of QDs probes and the suitable emission filters, holding great potential in biomedical research and non-invasive clinical diagnosis.

Declaration of competing interest

The authors declare that they have no known competing financial interests or personal relationships that could have appeared to influence the work reported in this paper.

CRediT authorship contribution statement

Fei Ma: Conceptualization, Writing - original draft. **Su Jiang:** Investigation, Writing - original draft. **Chun-yang Zhang:** Conceptualization, Funding acquisition, Writing - review & editing.

Acknowledgments

This work was supported by the National Natural Science Foundation of China (Grant Nos. 21735003, 21527811 and 21705096) and the Award for Team Leader Program of Taishan Scholars of Shandong Province, China.

Appendix A. Supplementary data

Supplementary data to this article can be found online at https://doi.org/10.1016/j.bios.2020.112177.

References

Baker, M.B., Bao, G., Searles, C.D., 2011. Nucleic Acids Res. 40 e13-e13.
Bartel, D.P., 2004. Cell 116, 281–297.
Bhuyan, A.K., 2010. Biopolymers 93, 186–199.
Calin, G.A., Croce, C.M., 2006. Canc. Res. 66, 7390–7394.
Chong, S., Mersha, F.B., Comb, D.G., Scott, M.E., Landry, D., Vence, L.M., Perler, F.B., Benner, J., Kucera, R.B., Hirvonen, C.A., Pelletier, J.J., Paulus, H., Xu, M.-Q., 1997. Gene 192, 271–281.
Chu, J., Oh, Y., Sens, A., Ataie, N., Dana, H., Macklin, J.J., Laviv, T., Welf, E.S., Dean, K. M., Zhang, F., Kim, B.B., Tang, C.T., Hu, M., Baird, M.A., Davidson, M.W., Kay, M.A., Fiolka, R., Yasuda, R., Kim, D.S., Ng, H.-L., Lin, M.Z., 2016. Nat. Biotechnol. 34, 760–767.
Deng, R., Zhang, K., Li, J., 2017. Acc. Chem. Res. 50, 1059–1068.
Geißler, D., Charbonnière, L.J., Ziessel, R.F., Butlin, N.G., Löhmannsröben, H.-G., Hildebrandt, N., 2010. Angew. Chem. Int. Ed. 49, 1396–1401.
Hébert, S.S., De Strooper, B., 2009. Trends Neurosci. 32, 199–206.
Habbe, N., Koorstra, J.-B.M., Mendell, J.T., Offerhaus, G.J., Ryu, J.K., Feldmann, G., Mullendore, M.E., Goggins, M.G., Hong, S.-M., Maitra, A., 2009. Canc. Biol. Ther. 8, 340–346.
Han, M., Gao, X., Su, J.Z., Nie, S., 2001. Nat. Biotechnol. 19, 631–635.
Hildebrandt, N., Spillmann, C.M., Algar, W.R., Pons, T., Stewart, M.H., Oh, E., Susumu, K., Díaz, S.A., Delehanty, J.B., Medintz, I.L., 2017. Chem. Rev. 117, 536–711.
Ho, Y.-P., Kung, M.C., Yang, S., Wang, T.-H., 2005. Nano Lett. 5, 1693–1697.

Hu, J., Liu, M.-h., Zhang, C.-y., 2018. Chem. Sci. 9, 4258–4267.
Huntzinger, E., Izaurralde, E., 2011. Nat. Rev. Genet. 12, 99–110.
Jaiswal, J.K., Mattoussi, H., Mauro, J.M., Simon, S.M., 2003. Nat. Biotechnol. 21, 47–51.
Kantharidis, P., Wang, B., Carew, R.M., Lan, H.Y., 2011. Diabetes 60, 1832–1837.
Kilic, T., Erdem, A., Ozsoz, M., Carrara, S., 2018. Biosens. Bioelectron. 99, 525–546.
Kroh, E.M., Parkin, R.K., Mitchell, P.S., Tewari, M., 2010. Methods 50, 298–301.
Li, J., Tan, S., Kooger, R., Zhang, C., Zhang, Y., 2014. Chem. Soc. Rev. 43, 506–517.
Liu, X.-G., Zhu, W.-Y., Huang, Y.-Y., Ma, L.-N., Zhou, S.-Q., Wang, Y.-K., Zeng, F., Zhou, J.-H., Zhang, Y.-K., 2012. Med. Oncol. 29, 618–626.
Ma, F., Li, Y., Tang, B., Zhang, C.-y., 2016. Acc. Chem. Res. 49, 1722–1730.
Ma, F., Zhang, Q., Zhang, C.-y., 2019. Nano Lett. 19, 6370–6376.
Medintz, I.L., Uyeda, H.T., Goldman, E.R., Mattoussi, H., 2005. Nat. Mater. 4, 435–446.
Mitchell, P.S., Parkin, R.K., Kroh, E.M., Fritz, B.R., Wyman, S.K., Pogosova-Agadjanyan, E.L., Peterson, A., Noteboom, J., O'Briant, K.C., Allen, A., Lin, D.W., Urban, N., Drescher, C.W., Knudsen, B.S., Stirewalt, D.L., Gentleman, R., Vessella, R. L., Nelson, P.S., Martin, D.B., Tewari, M., 2008. Proc. Natl. Acad. Sci. U.S.A. 105, 10513–10518.
Porkka, K.P., Pfeiffer, M.J., Waltering, K.K., Vessella, R.L., Tammela, T.L.J., Visakorpi, T., 2007. Canc. Res. 67, 6130–6135.
Qiu, X., Hildebrandt, N., 2015. ACS Nano 9, 8449–8457.
Resch-Genger, U., Grabolle, M., Cavaliere-Jaricot, S., Nitschke, R., Nann, T., 2008. Nat. Methods 5, 763–775.
Shen, Y., Tian, F., Chen, Z., Li, R., Ge, Q., Lu, Z., 2015. Biosens. Bioelectron. 71, 322–331.
Si, M.L., Zhu, S., Wu, H., Lu, Z., Wu, F., Mo, Y.Y., 2007. Oncogene 26, 2799–2803.
Silhavy, D., Molnár, A., Lucioli, A., Szittya, G., Hornyik, C., Tavazza, M., Burgyán, J., 2002. EMBO J. 21, 3070–3080.
Song, E., Yu, M., Wang, Y., Hu, W., Cheng, D., Swihart, M.T., Song, Y., 2015. Biosens. Bioelectron. 72, 320–325.
Stanisavljevic, M., Krizkova, S., Vaculovicova, M., Kizek, R., Adam, V., 2015. Biosens. Bioelectron. 74, 562–574.
Thomson, J.M., Parker, J., Perou, C.M., Hammond, S.M., 2004. Nat. Methods 1, 47–53.
Thum, T., Gross, C., Fiedler, J., Fischer, T., Kissler, S., Bussen, M., Galuppo, P., Just, S., Rottbauer, W., Frantz, S., Castoldi, M., Soutschek, J., Koteliansky, V., Rosenwald, A., Basson, M.A., Licht, J.D., Pena, J.T.R., Rouhanifard, S.H., Muckenthaler, M.U., Tuschl, T., Martin, G.R., Bauersachs, J., Engelhardt, S., 2008. Nature 456, 980.
Vargason, J.M., Szittya, G., Burgyán, J., Hall, T.M.T., 2003. Cell 115, 799–811.
Wang, Y., Zheng, D., Tan, Q., Wang, M.X., Gu, L.-Q., 2011. Nat. Nanotechnol. 6, 668–674.
Wienholds, E., Kloosterman, W.P., Miska, E., Alvarez-Saavedra, E., Berezikov, E., de Bruijn, E., Horvitz, H.R., Kauppinen, S., Plasterk, R.H.A., 2005. Science 309, 310–311.
Xu, P., Vernooy, S.Y., Guo, M., Hay, B.A., 2003. Curr. Biol. 13, 790–795.
Yang, Y., Zhang, C.-y., 2013. Angew. Chem. Int. Ed. 52, 691–694.
Ye, K., Malinina, L., Patel, D.J., 2003. Nature 426, 874–878.
Yi, R., Poy, M.N., Stoffel, M., Fuchs, E., 2008. Nature 452, 225–229.
Yin, B.-C., Liu, Y.-Q., Ye, B.-C., 2012. J. Am. Chem. Soc. 134, 5064–5067.